Coastal downwelling intensifies landfalling hurricanes

Supporting Information

Lewis J. Gramer[1,2,*], Jun A. Zhang[1,2], Ghassan Alaka[2], Andrew Hazelton[1,2], Sundararaman Gopalakrishnan[2]

[1] - Cooperative Institute for Marine and Atmospheric Studies, Miami, FL 33149.
[2] - NOAA Atlantic Oceanographic and Meteorological Lab, Miami, FL 33149.

[*] - Corresponding author: Dr. Lewis J. Gramer, 8930 Caribbean Blvd., Cutler Bay, FL 33157. Email: lew.gramer@noaa.gov. Telephone: +1-305-772-7933. ORCID: https://orcid.org/0000-0003-4772-1991

SUBMITTED: Oct 14, 2021
REVISIONS SUBMITTED: Feb 8, 2022

Supporting Information

Additional Details on Methods

The model in these case studies was the quasi-operational Basin-scale HWRF (HWRF-B; Zhang et al. 2016; Alaka et al. 2017, 2019, 2020) developed under HFIP. This model uses a fixed outer domain at 13.5 km horizontal resolution, with two TC-following nested domains at 4.5 and 1.5 km resolution, respectively. Up to five sets of nested domains can be deployed for a given initialization time to produce high-resolution forecasts for multiple TCs in the North Atlantic and eastern North Pacific. HWRF-B is coupled to MPIPOM-TC, an instance of the Princeton Ocean Model for TCs (Yablonsky et al. 2015) initialized with a two-day spinup from the Real-Time Ocean Forecasting System (RTOFS; Mehra and Rivin 2010).

Three TC case studies from the 2020 North Atlantic hurricane season were evaluated: Sally, Hanna, and Eta. Each TC experienced intensification while approaching land and interacted with the ocean shelf for a period of one day or more. To elucidate processes leading to intensification, model sea-surface fields were analyzed at forecast hours before and immediately after intensification. Supporting Information Table S1 details forecast initialization times for each case and forecast hours chosen for detailed analysis: the forecast hour immediately following intensification and a forecast hour prior to intensification that was near the peak of both air-sea flux and storm kinetic energy (see below). We evaluated the initialization and evolution of currents and sea temperatures over the shelf in MPIPOM-TC using quality-controlled buoy observations from the NOAA National Data Buoy Center (NDBC 2009; Winant et al. 1994) for one of the case studies, that for TC Sally.

We examined the relationship of air-sea fluxes to total storm kinetic energy and frictional dissipation using a model energy budget following Trenberth (1997) and Kato et al. (2016). Our Equation S1 is the result of integrating Trenberth's (1997) Eq. 16 over the inner TC domain.

$$\left[\iint\int_0^{p_s} KE\ dp\ dA\right]_{t0}^{tH} + \int_{t0}^{tH}\iint\int_0^{p_s} \nabla_p \cdot \vec{\boldsymbol{U}}\ KE\ dp\ dA\ dt - \left[\iint\int_0^{p_s} (c_pT + Lq + \Phi_s) dp\ dA\right]_{t0}^{tH}$$
$$- \int_{t0}^{tH}\iint\int_0^{p_s} \nabla_p \cdot \vec{\boldsymbol{U}}(c_pT + Lq + \Phi) dp\ dA\ dt + g\ RHF + g\ (THF_d + THF_s) - FD = 0 \qquad (1)$$

Eq. S1 includes terms for air pressure p, surface air pressure p_s, kinetic energy KE, storm domain area element A, forecast initialization time t_0 and forecast valid time t_H, wind velocity $\boldsymbol{U}^{\rightarrow}$, specific heat capacity of air c_p, air temperature T, latent heat of evaporation L, specific humidity q, geopotential at the surface ϕ_s and throughout the storm ϕ, respectively, gravitational acceleration g, net radiative heat flux RHF, net turbulent air-sea enthalpy flux over deep water THF_d and over the shelf THF_s, and frictional dissipation FD at the surface. Area element A is taken to consist of the region of instantaneous 17.5 ms^{-1} (34 kt) winds within the innermost domain (e.g., Figure 1). Square brackets denote differences between instantaneous values evaluated at different forecast hours.

We follow Emanuel (1986) and Wang and Xu (2010) in considering a simplified version of the above energy budget consisting of only the terms highlighted in red. This simplified equation elucidates the relationship between TC intensity change and TC interaction with the ocean and allows for the analysis of surface enthalpy fluxes over the shelf as a separate contribution to the budget. This study considers turbulent air-sea enthalpy fluxes only at gridpoints where 10 m winds are 17.5 ms^{-1} or greater. Fluxes within atmospheric grid cells over ocean model topography of 150 m depth or less are summed in the THF_s term; all other air-sea enthalpy fluxes are accumulated in THF_d. Frictional dissipation (FD) is estimated from predicted 10 m wind speeds as per Kato et al. (2016). We calculate total kinetic energy averaged over all vertical levels in the inner atmospheric model domain. All other terms in Eq. S1 (terms in black) are treated as residuals.

Additional Figures

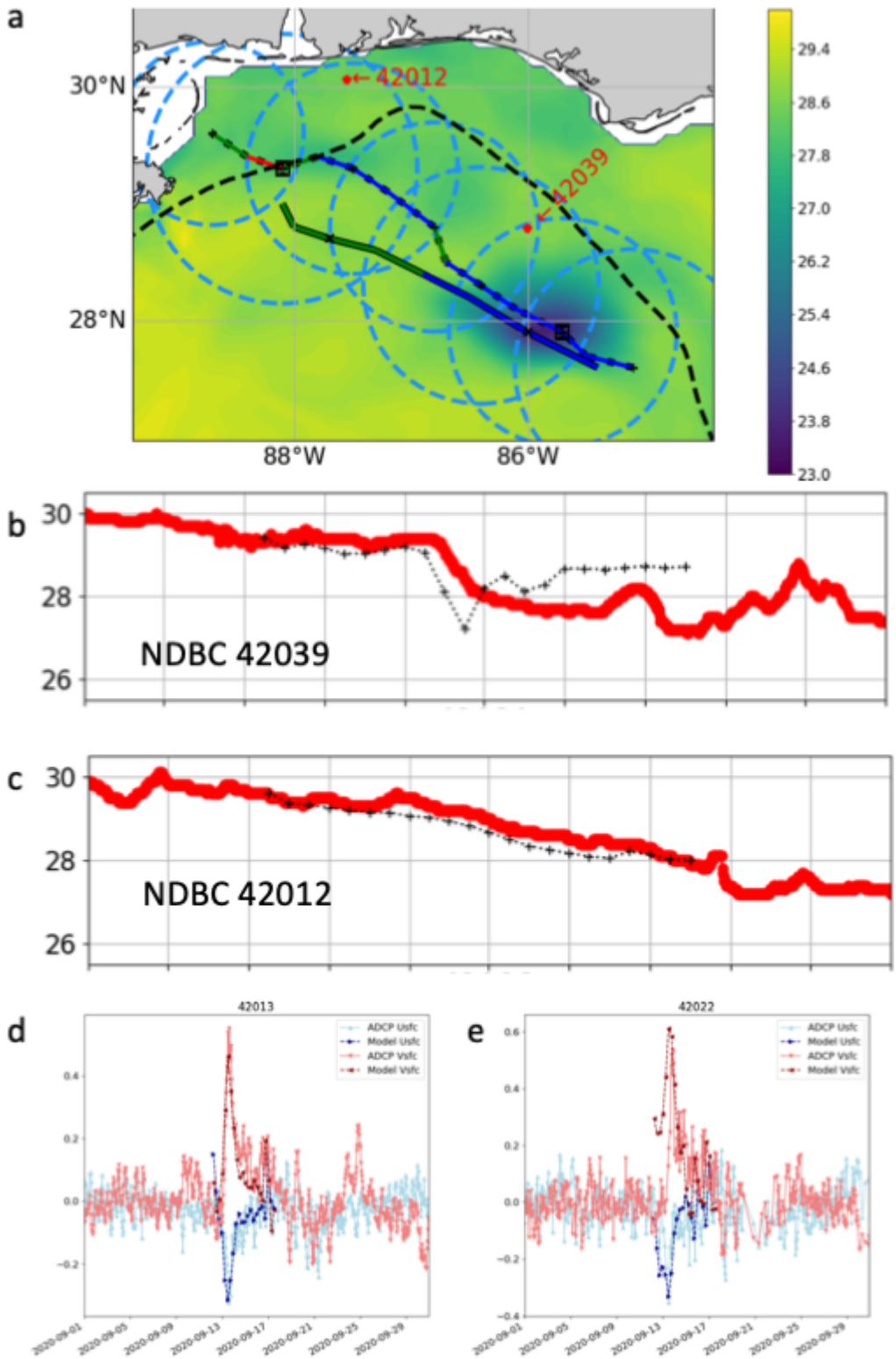

Figure S1: Data from NOAA NDBC buoys in the Gulf of Mexico for 10-20 Sep 2020: (a) map showing model SST for forecast hour 54, together with location of buoys (red dots) along Sally's HWRF-B forecast track (dashed outline, colored by storm intensity) and 17.5 ms^{-1} wind radii (circles). Best track is also outlined with solid black. Model 150 m isobath is a dashed black line.

(b) Near-surface sea temperature (red) compared with model SST (dotted black “+”) for buoy 42039 in the deeper Gulf, water depth 281 m. (c) Near-surface temperature and model SST for buoy 42012 on the northern Gulf shelf in 24 m of water. (d) Near-surface currents west-to-east across-shore (u, blue) and south-to-north alongshore (v, red); solid lines show quality-controlled ADCP measurements (top good bin) from two buoys on west Florida shelf, dashed lines ocean model output (top model level).

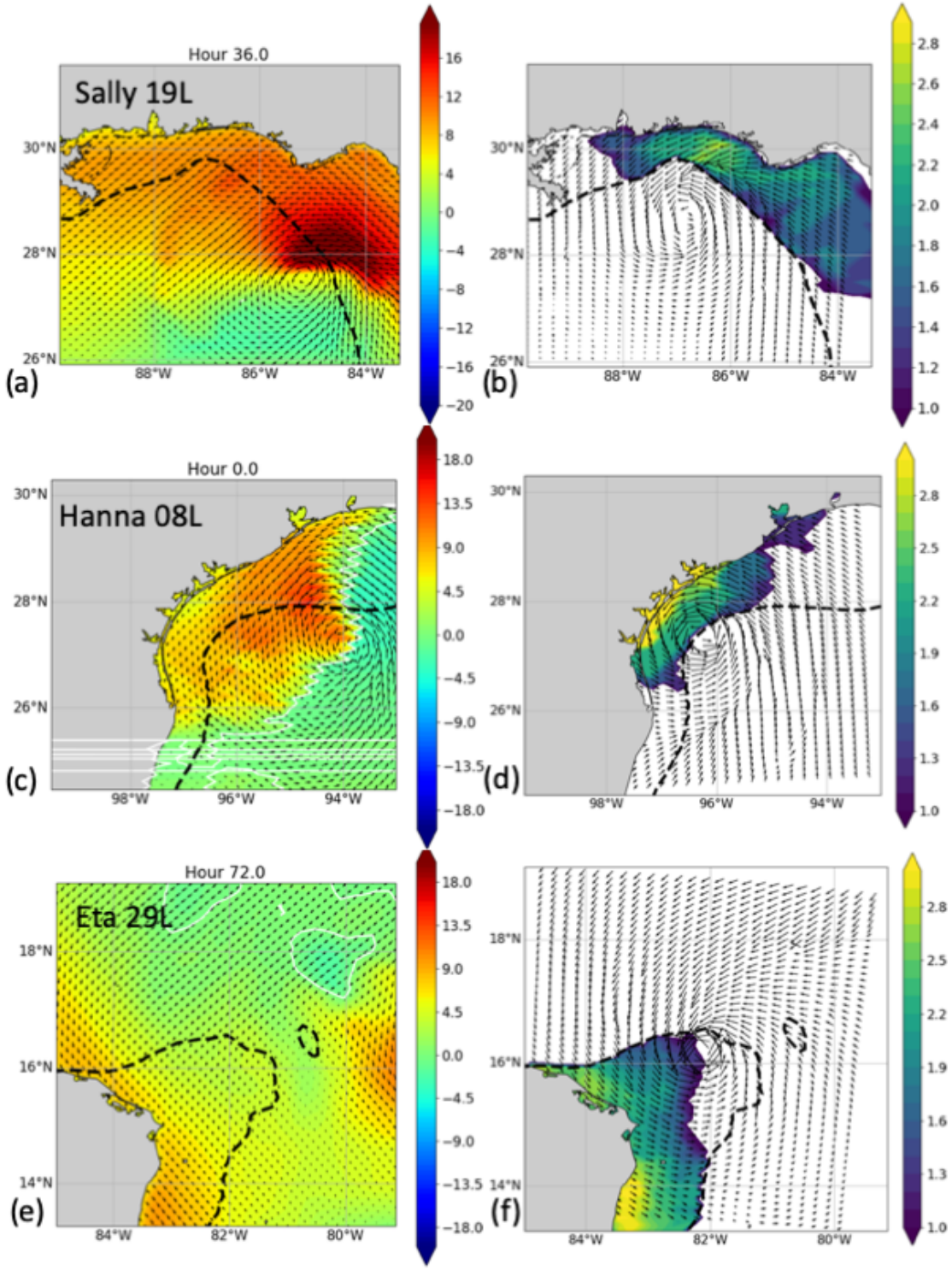

Figure S2: (a,c,e) Snapshot of wind vectors and magnitude of downwelling-favorable wind component (shading, zero contour marked in white) at a forecast hour one inertial period prior to intensification; (b,d,f) Wind vectors at hour just prior to intensification, and accumulated number of inertial periods (22 h at the latitude of Sally and Hanna, 42 h for Eta) during which downwelling-favorable winds were blowing over the shelf. Thick dashed black line shows the 150 m isobath outlining the shelf regions; land is in gray.

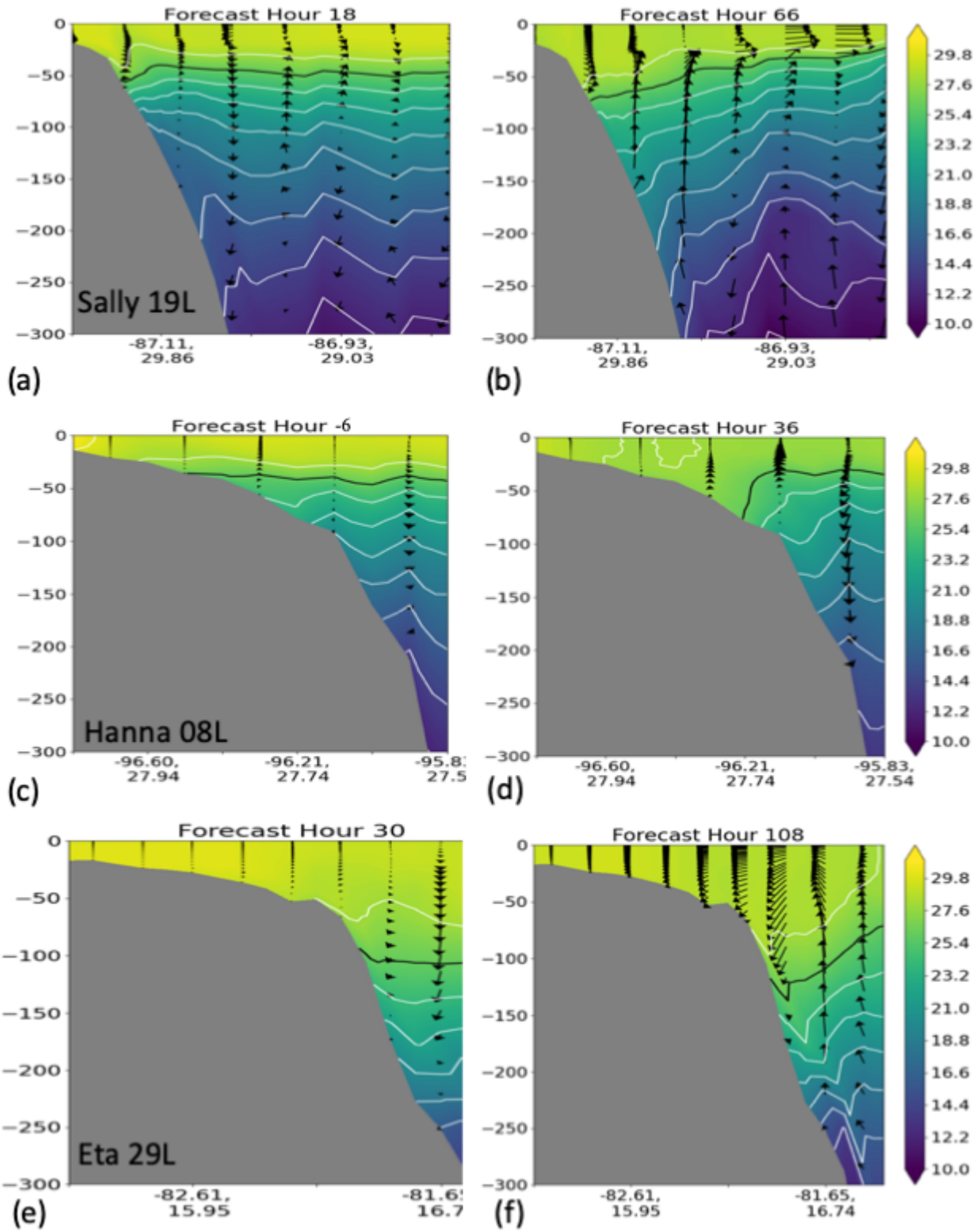

Figure S3: Section plots (along the same section lines shown in Figure 2, middle panel), shown here at two other times separated from each other by two local inertial periods. These show the evolution of the downwelling circulation cell and depression of isotherms over the shelf that formed ahead of the passage of each TC.

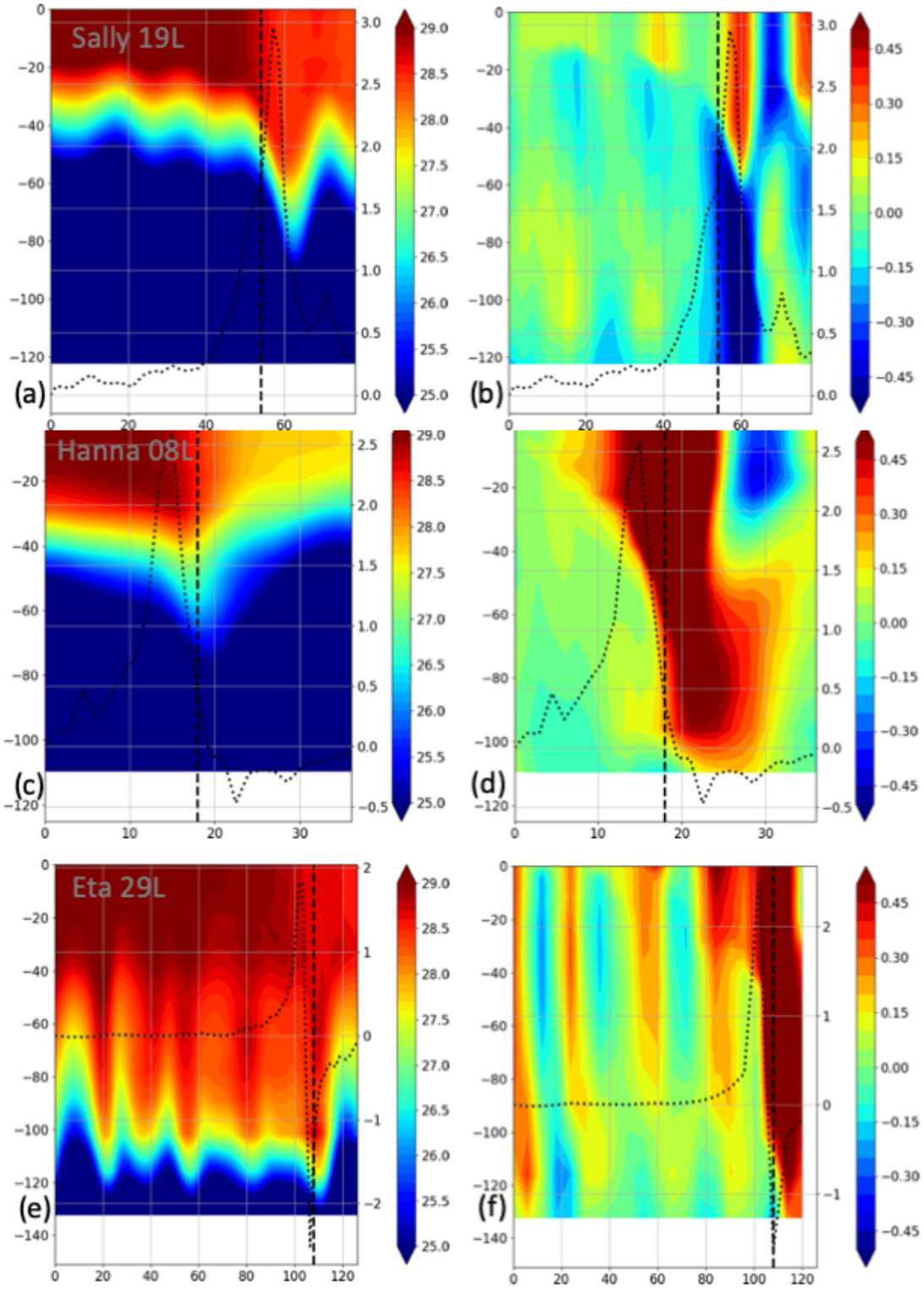

Figure S4: Hovmoeller diagrams showing change in vertical ocean profiles at a point near the 150 m isobath along each of the onshore tracks in the left and middle panels of Figure 2. (a,c,e) Ocean temperature and (b,d,f) cross-shelf currents. The right axis and black dotted line show along-shore 10 m wind stress from the model [N/m^2]. Dashed vertical black line shows the forecast hour highlighted in Figure 2 and in the left panels of Figures 1, 3, and 4.

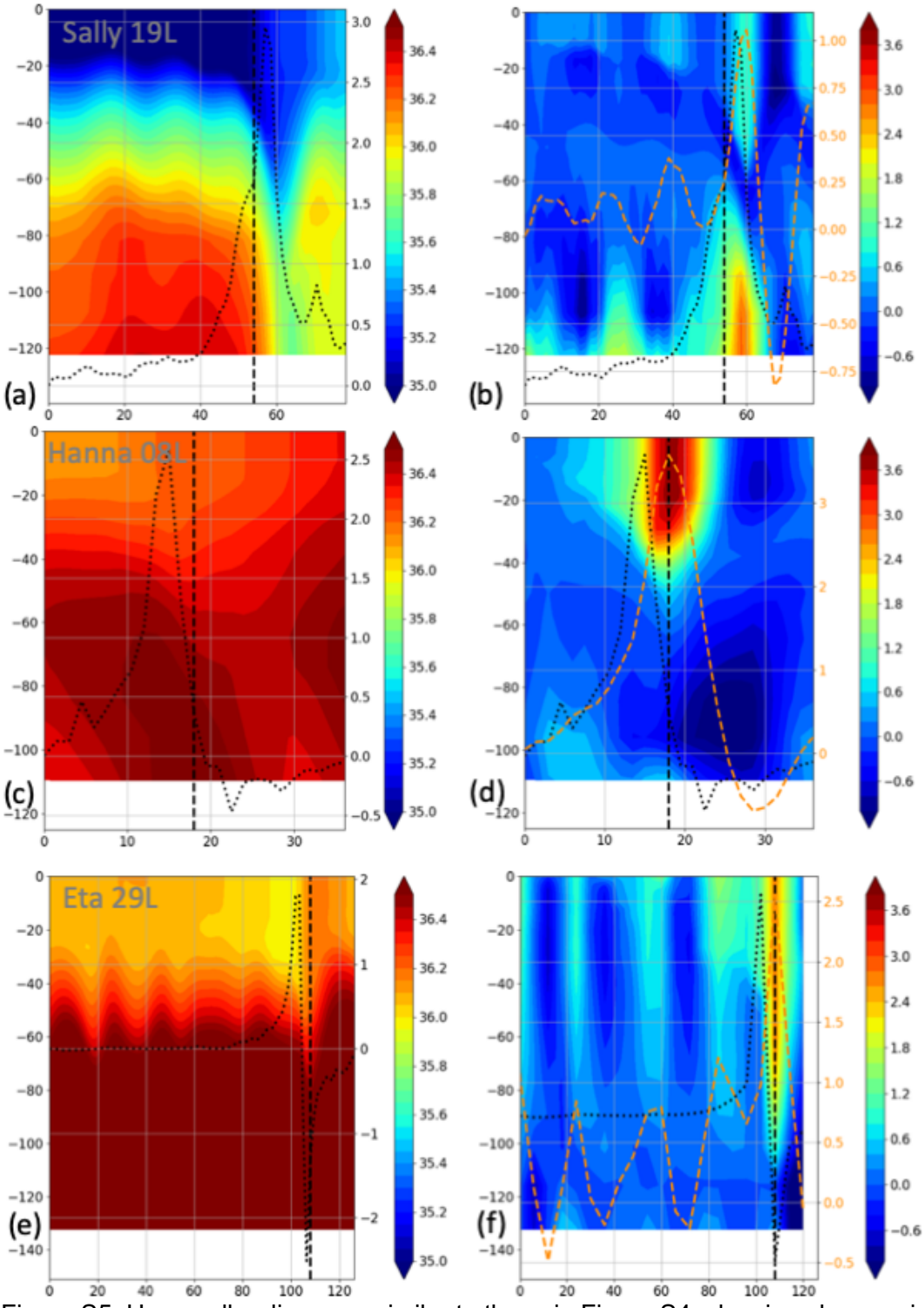

Figure S5: Hovmoeller diagrams similar to those in Figure S4, showing changes in: (a,c,e) salinity and (b,d,f) cross-shore heat transports. For left-hand panels, the right axis and black dotted line show along-shore 10 m wind stress from the model [N/m^2]. For right-hand panels, black dotted line still shows along-shore wind stress but with no corresponding axis, while the dashed orange line and right axis show cross-shore net heat flux [MW/m^2] relative to 26 °C.

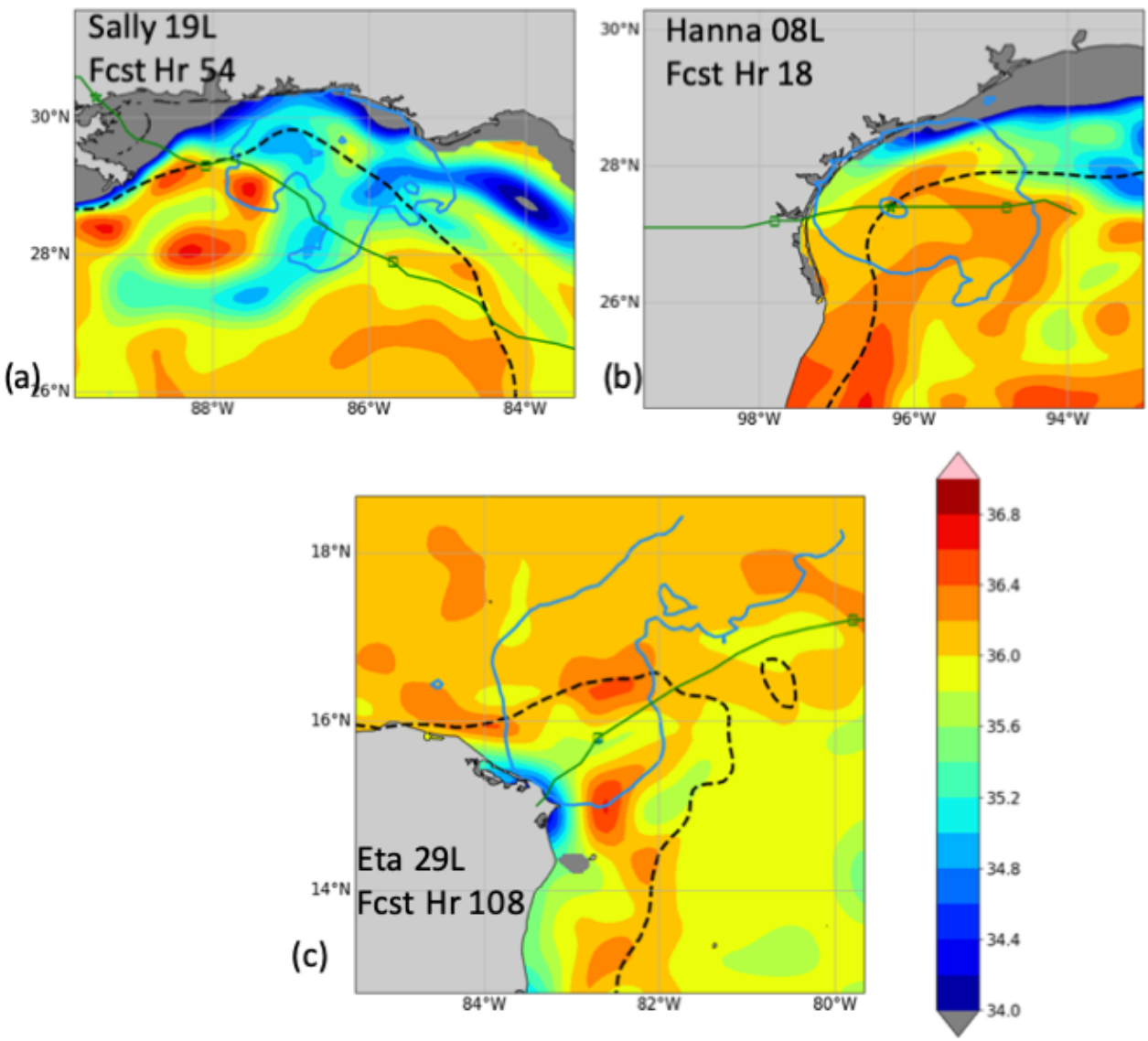

Figure S6: Model sea-surface salinity (shading) at forecast hour just prior to intensification for each of the three case studies. Contour of winds > 17.5 m/s (blue) and the 150 m isobath (black dashed), and forecast TC track and positions (green lines and squares) as in Figures 1-3.

Table S1: Storm forecast initialization time, forecast hours (chosen before and after intensification) that are highlighted in Figs.1-4, peak intensity change in the 24 h following the first highlighted forecast hour, and environmental characteristics during the highlighted period: environmental deep vertical wind shear (200-850 mbar), translation speed of the storm, total air-sea enthalpy flux (THF), and percentage of THF deriving from shelf waters.

Storm	**Forecast Init. Time**	**Fcst. Hours Highlighted**	**Forecast Intensity Change in 24 h; ms^{-1}**	**Environ. Shear; ms^{-1}; Direction**	**Fcst. Storm Transl. Speed; ms^{-1}; Dir.**	**Total Air-Sea Heat Flux (THF); TJ**	**% THF from shelf**
Sally 19L	0600Z 12 September 2020	54, 66	+26	13 WSW	3.0 SE	$1.0x10^7$	60%
Hanna 08L	1800Z 24 July 2020	18, 24	+18	5.1 NW	4.1 E	$3.5x10^6$	80%
Eta 29L	0600Z 30 October 2020	108, 114	+11	8.7 S	3.6 NE	$1.8x10^7$	40%